

Onset Characteristics of Aqueous Electrospays

Adrian Ieta¹, *Member, IEEE*, Dennis Quill¹, and Thomas E. Doyle², *Member, IEEE*

¹*Department of Physics, State University of New York at Oswego, NY, USA, email: ieta@oswego.edu*

²*Electrical and Computer Engineering Department, McMaster University, Canada*

Abstract—Electrospays have a wide variety of applications. Particularly the onset voltage parameter is of special interest. In our study onset characteristics of aqueous electrospays were investigated in a negative polarity for capillary tip-plate distances in the range of 0.5 cm to 50 cm. Experimental work shows a significant variation of the onset voltage with the presence of metallic objects in the proximity of the electrospay. Data analysis shows an increase in onset voltage with the decrease in counter electrode radius. The region least sensitive to such variation was found for tip-plate distances larger than 20 cm. Onset voltages appear to be in agreement with Smith's formula for a certain range of the distance studied. Gaps larger than 25 cm have generally showed more significant variations of this formula. The results of the present study can be useful for the design of electrospays of larger gaps.

Index Terms—aqueous electrospay, charged droplets, electrospay control, onset voltage, Smith's formula

I. INTRODUCTION

When high voltage is applied to a conductive capillary/needle containing a polar fluid, an electrospay can be generated. As voltage increases, the liquid air interface becomes polarized with an excess ionic charge producing Taylor's cones [1, 2], which are not yet completely understood [3]. Charge droplets emitted at the tip of Taylor's cone undergo coulombic fissions around Rayleigh limit [4, 5, 6]. The droplets evaporate and pass through a succession of coulombic fissions as they move towards the counter electrode.

Various electrospay regimes are described in the literature [7-9].

The variety of variables affecting an electrospay often makes it difficult to investigate and predict its operation; among the variable categories are voltage, liquid flow, electrode geometry, and physical properties of the liquid [3]. As the spray develops it may or may not be accompanied by corona discharge, which was identified as a trigger mechanism in the break-up of a current-driven jet [10]. In experiments with nanoelectrospay capillaries current pulsations were observed only after the onset of corona discharges [7]. Even for voltages lower than 5 kV a faint glow discharge may be observed [11]. The experiments suggest that the corona

discharge is from the whole surface of the liquid, specifically for conducting liquids such as water [12].

An obviously important parameter is the electrospay onset voltage. The onset voltage is not necessarily a precise voltage but rather a voltage range. The value of electrospay onset voltage is usually associated with a sharp rise in the value of the ES current [13]. The frequency of the emitted droplets in the transition from the dripping regime to spray appears to be characterized by a universal pattern [14]. The current-voltage characteristics present three rather distinct regions. Only in the relatively constant current region a stable Taylor cone and orderly generation of charged droplets can be observed [15]. For micrometer size capillaries currents are in the nanoampere range at the onset voltage [16]. A steep rise in current (mA) may develop at much higher voltages but this is due mainly to the corona currents [12]. If pulsed voltages are superimposed on the dc voltages the onset and regimes are changed. Greater pulsed voltages were associated with jet formation [17].

The electrospay has been heavily researched lately, with particular focus on the stable cone-jet regime, which is relevant to the production of macromolecular ions and is used in conjunction with mass spectrometry in fundamental research involving biological molecules [4, 18-21]. In this regime the spray current is nearly independent of the nature and pressure of the surrounding gas [22]. However, there are other electrospay applications, such as electrostatic painting, drug delivery, drug micro-encapsulation, production of nanofibers, steering of micro-satellites, detection of trace explosives, thin film deposition [23], and powder production [24]. Some applications involve larger capillary tip-plate gaps than required for the cone-jet regime. The purpose of our study, related to the latter cases, is to investigate the dependence of aqueous electrospay onset characteristics on the tip-plate gap and the surrounding

II. EXPERIMENTAL SETUP

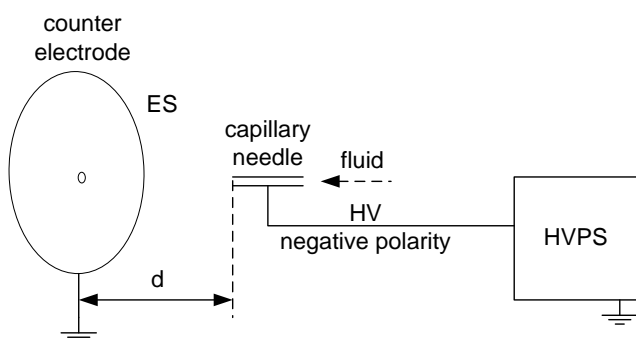


Fig. 1 Schematic of the Setup

A simplified version of the setup is shown in Fig. 1. The capillary nozzles were modified BD PrecisionGlide hypodermic syringe needles, regular wall type and regular bevel 25G x 1.5 in (ID 0.241 mm, OD 0.508 mm). The original needles were cut and polished in order to obtain blunt tips. Needles were attached to a 3 mL BD Luer-Lok™ syringe with positive plunger rod stop and tapered plunger rod design. In all the experiments a natural flow rate of the fluid (water) through the needle is ensured by constant differential hydrostatic pressure. The syringe was modified and connected to a plastic cylindrical container (18 cm diameter) by using clear vinyl tubing. A 14.5 cm long syringe adaptor was manufactured out of Polytetrafluoroethylene (Teflon) in order to attach the syringe to one end of a 1 m long rectangular rigid wood element (100 cm x 7 cm x 2 cm). The syringe system is attached to a wood table equipped with a ruler that permits the syringe system to glide along the table and parallel to the floor, 77.5 cm above the laboratory floor. Wood was the preferred material for our setup as it has a much lower influence on the onset voltage than metal objects do.

The polar fluid used in our experiments is water, known to have a relatively high surface tension [3] (72.8 mN/m at 20°C). The counter electrode consists of a circular metal plate axially sustained in a vertical position, coaxial with the needle. Three plates of different diameters are employed in our experiments (Table 1). The plates of 6 mm thickness have a central hole of 6.5 mm diameter, which allows for easy replacement of the plates on the plate holder (plate axis 78.3 cm above the floor). All reported measurements are performed with the plate grounded and the needle connected to the negative polarity of the high voltage. The plate position was fixed and the needle-plate distance was varied by sliding the syringe system. The high voltage is supplied by a high voltage power supply (HVPS) Glassman (50kV DC).

Due to the charging properties of the electro spray, the onset voltage is significantly influenced by the presence of metal objects around the electro spray system. In order to alleviate such effects, any metal objects were removed from the proximity of the capillary-plate system to a distance of at least 110 cm. All experiments were performed at atmospheric pressure and the needle-plate temperature was 26-27°C. Air

humidity varied between 40% and 50%.

TABLE I
ES COUNTER ELECTRODE RADII

Plate radius [cm]	R1	R3	R5
	3.8	7.85	12.7

The distance between the capillary needle and the metal plate can easily be controlled in the described setup. The ES onset voltage was initially recorded in small increments and the regions of interest and appropriate increments were chosen. As voltage is increased, the natural dripping frequency increases slowly while droplet size decreases. As voltage approaches onset voltage, the frequency of droplet emission increases. The ES onset voltage was marked where the dripping mode was indistinguishable from the continuous emission of water droplets. The constant hydrostatic pressure generating the natural water flow rate was 2638.9 N/m² corresponding to a 26.9 cm water column above the capillary needle level. The natural flow rate in the specified conditions (before the application of high voltage) was 0.45 ml/min for the 25G needle. The onset voltage was measured using the counter electrode plates of radii given in Table 1. Additional measurements were performed with no plate at all (only with the ground wire as counter electrode). The variation of onset voltage with distance from the tip of the capillary to the plate is showed in Fig. 2. The values of the ES onset voltage lie between the curve given by Plate 5 (the largest radius) and the dotted line of the “No Plate” measurements. As the tip-plate distance increases, the onset voltage increases so that the curves corresponding to different plates used converge about d=30 cm. Measurements close to the plate are likely affected by larger errors in identifying the onset voltage. This is mainly due to the fact that droplets stick to the counter electrode plate and can modify the local electric field by significantly changing the tip-plate distance percentage-wise.

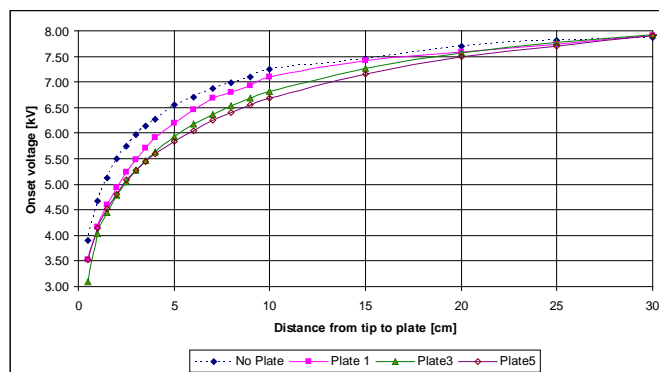


Fig. 2. Variation of the ES onset voltage with tip-plate distance.

We found that the symmetry of the electric field generated by the needle-plate configuration allows for a better comparison of the voltage – gap distance characteristics. If a geometrically specified point on the needle-plate axis is chosen as reference, then normalizing the voltage values to the reference voltage value gives natural grounds for comparison of the characteristics obtained for different plates. For symmetry

reasons we chose the reference point at a distance of $(/6)R$ from the plate along the needle-plate axis. The normalized onset voltage for the three plates used is given in Fig. 3. The normalized values show consistent increase in normalized voltage with the plate radius for all tip-plate distances with the smallest radius sensitivity in the proximity of the plate and highest at about 10 cm gap.

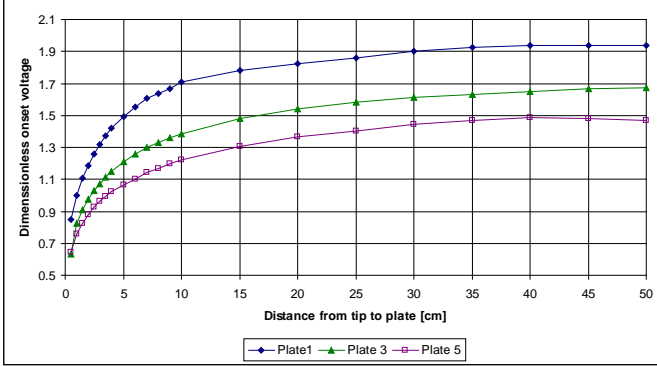


Fig. 3. Normalized onset voltages.

Voltage-distance characteristics for Plate 2 are shown in Fig. 4. The asymptotic variation of voltage with distance is apparent. The same voltage variation is shown in Fig. 5 in semilog coordinates. The linear variation of the voltage with the logarithm of the distance can be noticed for most of the studied distance range. The linearity does not appear to hold well for tip-plate gaps larger than 25 cm.

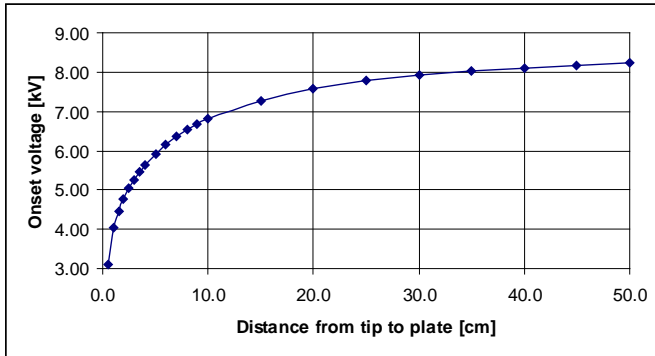


Fig. 4. Plate 2: variation of the ES onset voltage with tip-plate distance.

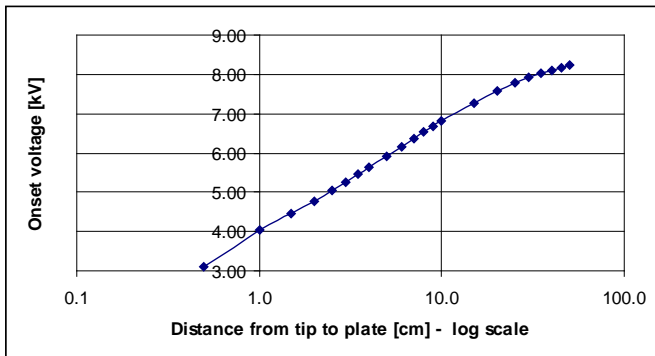


Fig. 5. Plate 2: variation of the ES onset voltage with tip-plate distance – semilog coordinates.

A comparison of normalized voltages is presented in Fig. 6. The log scale used for the gap distance again shows the linearity, within certain limits, of the onset voltage with tip-plate distance. The dotted lines represent the linear regressions corresponding to each data set. The oscillations of experimental data points about the regression line are more pronounced for the smallest plate, indicating a less accurate linearity, particularly beyond the 25 cm region. Some of the fluctuations may be related to measurement errors associated with the identification of onset voltage. However, experimental data trends are consistent for all the plates, likely revealing variations due to change in plate radius. The slope of regression lines consistently increases with the decrease in plate radius. The trend suggests that the normalized voltage – gap characteristics may be bound by the no plate (virtually zero radius) characteristic with the highest slope and the infinite radius plate with the lowest slope.

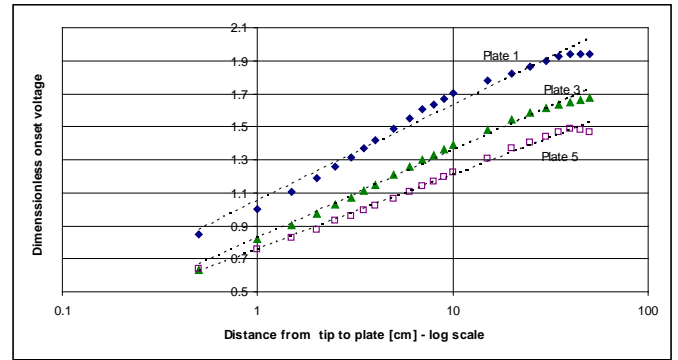


Fig. 6. Comparison of normalized onset voltages for different plate radii.

II. DISCUSSION

A relation giving the dependence of onset voltage V_{on} was shown by Smith [25] and used by others [26, 27] to explain parametric dependence of ES. The relation is derived from balancing the condition of electric field and surface tension forces:

$$V_{on} = A \left(\frac{\gamma \cdot \cos \theta \cdot r_c}{\epsilon_0} \right)^{1/2} \ln \frac{4d}{r_c} \quad (1)$$

where γ is the surface tension of the fluid, θ the half angle of the liquid cone at the tip of the capillary, r_c the outer radius of the capillary, ϵ_0 the electric permittivity of vacuum, and A a proportionality constant.

Relation (1) can be rewritten as

$$V_{on} = A \left(\frac{\gamma \cdot \cos \theta \cdot r_c}{\epsilon_0} \right)^{1/2} \ln \frac{4}{r_c} + A \left(\frac{\gamma \cdot \cos \theta \cdot r_c}{\epsilon_0} \right)^{1/2} \ln d \quad (2).$$

Given that in our experiments r_c , γ , θ are constants, relation (2) can be simplified to

$$V_{on}(d) = a \ln d + b \quad (3)$$

With

$$a = A \left(\frac{\gamma \cdot \cos \theta \cdot r_c}{\epsilon_0} \right)^{1/2} \text{ and}$$

$$b = A \left(\frac{\gamma \cdot \cos \theta \cdot r_c}{\epsilon_0} \right)^{1/2} \ln \frac{4}{r_c}. \quad (4)$$

Hence, the variation of onset voltage with the logarithm of tip-plate distance should be linear. The experimental data plotted in Fig. 6 and Fig. 7 confirm the predictions of relation (3) to a good extent. Logarithmic regressions of experimental data give a fit with an R^2 of 0.997 for Plate 3 (the largest radius) decreasing to 0.97 for “no plate” measurements. Relation (1) appears to be in fair agreement with our experimental data. Deviations from the predictions of this relation appear at shorter distances as the radius of the electrode plate is decreased.

An average electric field $E = V_{on}/d$ was calculated and scaled to its value for a reference point as previously defined $E^* = V^*/d^*$ (V^* is the onset voltage corresponding to reference distance d^*). Comparison of the normalized electric field for different plate radii counter electrodes is shown in Fig. 8. The linear variation of the field with the tip-plate distance is evident in log coordinates for the studied range. The normalized electric field increases with plate radius. The curves corresponding to the three plate electrodes exhibit a linear variation of the field with distance in logarithmic coordinates and the associated linear regressions are virtually the same.

The observed linearity also appears to be explained by Smith's relation (1). Experimental data plotted in Fig. 7 suggest that

$$\ln E = \ln \frac{V_{on}}{d} = a_0 \ln d + b_1 \quad (5)$$

where a_0 and b_1 are experimentally determined constants. Hence

$$\ln V_{on} = (1 + a_0) \ln d + b_1 = a_0' \ln d + b_1 \quad (6)$$

where $a_0 + 1 = a_0'$. Relation (6) is similar to (3), in agreement with Smith's formula.

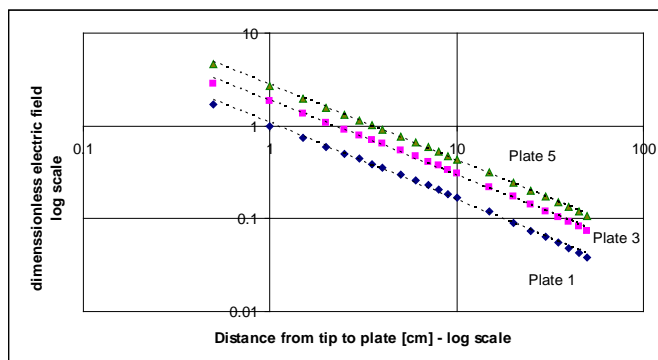


Fig. 7. Average electric field corresponding to onset voltage as a function of tip-plate gap.

III. CONCLUSIONS

Onset characteristics of aqueous electrospays were investigated in a negative polarity for capillary tip-plate distances in the range of 0.5 cm to 50 cm. Experimental work shows a significant variation of the onset voltage with the presence of metallic objects in the proximity of the electrospay. A distance larger than 100 cm was found to be limiting onset voltage variations to a non-significant level. Data analysis shows an increase in onset voltage with the decrease in counter electrode radius. The region least sensitive to such variation was found for tip-plate distances larger than 20 cm. The onset voltage appears to be in agreement with Smith's formula (1) for about half of the distance range studied. The correspondence of experimental data to Smith's formula was also evidenced by the analysis of a normalized average electric field in the gap. Gaps larger than 25 cm have generally showed more significant variations of this formula, which were more intense with the decrease in counter electrode radius. We believe that the results of the present study can be useful for the design of aqueous electrospays of larger gaps.

ACKNOWLEDGMENT

The authors are thankful to Hunter Gerlach for his contribution with laboratory measurements.

REFERENCES

- [1] Robinson, James A. "Quasi Taylor Cones" Generated by AC Fields on Water Surfaces. Ph.D. dissertation, The University of Western Ontario, London, Ontario, Canada, 2000.
- [2] Gamero-Castaño, M., and V. Hruby. "Electrospray as a source of nanoparticles for efficient colloid thrusters." *J. Propulsion and Power* 17.5 (2001): 977.
- [3] de la Mora, J. F. "The fluid dynamics of Taylor cones." *Annual Review of Fluid Mechanics* 39 (2007): 217-243.
- [4] Gomez, A., and K. Q. Tang. "Charge and fission of droplets in electrostatic sprays." *Physics of Fluids* 6.1 (1994): 404-14.
- [5] Li, K. Y., H. H. Tu, and A. K. Ray. "Charge limits on droplets during evaporation." *Langmuir* 21.9 (26 April 2005): 3786-3794.
- [6] Duft, D., T. Achtzehn, R. Muller, et al. "Coulomb fission - Rayleigh jets from levitated microdroplets." *Nature* 421.6919 (2003): 128.
- [7] Juraschek, R., and F. W. Rollgen. "Pulsation phenomena during electrospay ionization." *International Journal of Mass Spectrometry* 177.1 (3 August 1998): 1-15.
- [8] Jaworek, A., and A. Krupa. "Classification of the modes of EHD spraying." *Journal of Aerosol Science* 30.7 (August 1999): 873-893.
- [9] Marginean, I., P. Nemes, and A. Vertes. "Astable regime in electrospays." *Physical Review* 76.2 (August 2007): Art. No. 026320, Part 2.
- [10] Hoburg, J.F., J.R Melcher, "Current-driven, corona-terminated water jets as sources of charged droplets and audible noise." *IEEE Transactions on Power Apparatus and Systems*, PA94.1 (1975): 128-136
- [11] Jaworek, A., T. Czech, E. Rajch, M. Lackowski. "Spectroscopic studies of electric discharges in electrospaying" *Journal of Electrostatics*, 63 (2005) 635-641.
- [12] Jaworek, A. and A. Krupa. "Studies of the corona discharge in ehd spraying" *Journal of Electrostatics*, 40 & 41 (1997) 173-178.
- [13] Arscott, S and D. Troadec. "Electrospraying from nanofluidic capillary slot" *Applied Physics Letters* 87, (2005) 134101
- [14] Ieta, A. Gerlach, H, Doyle, T.E., Pallone, A., and Amundson, R. "Scaling Law for Electrospay Droplet Formation" *Particulate Science and Technology* (in print 2009)
- [15] Cech, N. B. "Practical implications of some recent studies in electrospay ionization fundamentals." *Mass Spectrometry Reviews* 20 (2001): 362-387.

- [16] Schmidt, A. and M. Karas. "Effect of different solution flow rates on analyte ion signals in nano-ESI MS, or: When does ESI turn into Nano-ESI?" *Journal of the American society for mass spectrometry*, 14.5 (2003): 492-500
- [17] Li, J.L. "EHD sprayings induced by the pulsed voltage superimposed to bias voltage." *Journal of Electrostatics*, 65 (1997) 750-757.
- [18] Manisali, Irina, David D. Y. Chen, and Bradley B. Schneider. "Electrospray ionization source geometry for mass spectrometry: past, present, and future." *Trends in Analytical Chemistry* 25.3 (2006): 243-56.
- [19] Fenn, John B. "Electrospray Wings for Molecular Elephants (Nobel Lecture)." *Angew. Chem. Int. Ed.* 42 (2003): 3871-94.
- [20] Takats, Zoltan, Justin M. Wiseman, Bogdan Gologan, and R. Graham Cooks. "Mass spectrometry sampling under ambient conditions with desorption electrospray ionization." *Science* 306 (15 October 2004): 471-3.
- [21] Cooks, R. G., Z. Ouyang, Z. Takats, et al. "Ambient mass spectrometry." *Science* 311.5767 (17 March 2006): 1566-1570.
- [22] Aguirredecacer, I. and J.F. Delamora. "Effect of background gas on the current emitted from Taylor cones" *Journal of colloid and interface science*, 171.2 (1995): 512-517.
- [23] Jaworek A. "Electrospray droplet sources for thin film deposition." *Journal of Materials Science* 42.1 (2007): 266-297.
- [24] Jaworek, A. "Micro- and nanoparticle production by electrospraying." *Powder Technology* 176 (2007): 18-35.
- [25] Smith, D. P. H. "The electrohydrodynamic atomization of liquids." *IEEE Transactions on Industry Applications* 22 (1986): 527-535.
- [26] Ikonou, M. G., A. T. Blades, and P. Kebarle. "Electrospray mass spectrometry of methanol and water solutions suppression of electric discharge with SF₆ gas." *Journal of American Society for Mass Spectrometry* 2 (1991): 497-505.
- [27] Wei, J. F., W. Q. Shui, F. Zhou, Y. Lu, K. K. Chen, G. B. Xu, and P. Y. Yang. "Naturally and externally pulsed electrospray." *Mass Spectrometry Reviews* 21 (2002): 148-162.